



Published in final edited form as:

*J Bone Miner Res.* 2016 May ; 31(5): 929–939. doi:10.1002/jbmr.2783.

## 1,25-dihydroxyvitamin D alone improves Skeletal Growth, Microarchitecture and Strength in a Murine model of XLH, despite enhanced FGF23 expression

Eva S. Liu<sup>1,2,3</sup>, Janaina S. Martins<sup>2,3,4</sup>, Adalbert Raimann<sup>2,3,5</sup>, Byongsoo Timothy Chae<sup>2</sup>, Daniel J. Brooks<sup>2,6</sup>, Vanda Jorgetti<sup>4</sup>, Mary L. Bouxsein<sup>2,3,6</sup>, and Marie B. Demay<sup>2,3</sup>

<sup>1</sup>Division of Endocrinology, Diabetes, and Hypertension, Brigham and Women's Hospital, Boston, Massachusetts 02115

<sup>2</sup>Endocrine Unit, Massachusetts General Hospital, Boston, Massachusetts 02114

<sup>3</sup>Harvard Medical School, Boston, Massachusetts 02115

<sup>4</sup>Division of Nephrology, Universidade de São Paulo, São Paulo, Brazil

<sup>5</sup>Department of Pediatrics and Adolescent Medicine, Medical University Vienna, Vienna, Austria

<sup>6</sup>Department of Orthopedics, Beth Israel Deaconess Medical Center, Boston, MA 02115

### Abstract

X-linked hypophosphatemia (XLH) is characterized by impaired renal tubular reabsorption of phosphate due to increased circulating FGF23 levels, resulting in rickets in growing children and impaired bone mineralization. Increased FGF23 decreases renal brush border membrane sodium-dependent phosphate transporter IIa (Npt2a) causing renal phosphate wasting, impairs 1- $\alpha$  hydroxylation of 25-hydroxyvitamin D and induces the vitamin D 24-hydroxylase leading to inappropriately low circulating levels of 1,25-dihydroxyvitamin D (1,25D). The goal of therapy is prevention of rickets and improvement of growth in children by phosphate and 1,25D supplementation. However, this therapy is often complicated by hypercalcemia and nephrocalcinosis, and does not always prevent hyperparathyroidism. To determine if 1,25D or blocking FGF23 action can improve the skeletal phenotype without phosphate supplementation, mice with XLH (Hyp) were treated with daily 1,25D repletion, FGF23 antibodies (FGF23Ab), or biweekly high dose 1,25D from d2 to d75 without supplemental phosphate.

All treatments maintained normocalcemia, increased serum phosphate and normalized parathyroid hormone levels. They also prevented the loss of Npt2a,  $\alpha$ -Klotho and pERK1/2 immunoreactivity observed in the kidneys of untreated Hyp mice. Daily treatment with 1,25D decreased urine phosphate losses despite a marked increase in bone FGF23 mRNA and in circulating FGF23 levels. Daily 1,25D was more effective than other treatments in normalizing the growth plate and

---

Correspondence should be addressed to: Marie Demay, Endocrine Unit, Massachusetts General Hospital, 50 Blossom Street, Thier 11, Boston, MA 02114, Fax: 617-726-7543, Tel: 617-726-3273, demay@helix.mgh.harvard.edu.

All authors have declared that no conflict of interest exists.

Authors' roles: Project design: E.S.L. and M.B.D., Mouse colony management: E.S.L., A.R., and B.T.C., Molecular biology experiments and histological analyses: E.S.L., B.T.C., J.S.M., Serum analyses and cell culture experiments: E.S.L.,  $\mu$ CT and biomechanics: D.B., E.S.L., M.L.B., Histomorphometric analyses: J.S.M., V.J., Manuscript preparation: E.S.L., M.B.D.

metaphyseal organization. In addition to being the only therapy that normalized lumbar vertebral height and body weight, daily 1,25D therapy normalized bone geometry and was more effective than FGF23Ab in improving trabecular bone structure. Daily 1,25D and FGF23Ab improved cortical microarchitecture and whole-bone biomechanical properties more so than biweekly 1,25D. Thus, monotherapy with 1,25D improves growth, skeletal microarchitecture and bone strength in the absence of phosphate supplementation despite enhancing FGF23 expression, demonstrating that 1,25D has direct beneficial effects on the skeleton in XLH, independent of its role in phosphate homeostasis.

## Keywords

Genetic mouse models; PTH/VitD/FGF23; Growth plate; Bone QCT/ $\mu$ CT; Biomechanics

## Introduction

X-linked hypophosphatemia is the most common cause of hypophosphatemic rickets, with an incidence of 1:20,000 in the general population.<sup>(1)</sup> Affected children exhibit growth retardation associated with rickets and osteomalacia.<sup>(2)</sup> The genetic basis for this disorder is mutation of the PHEX endopeptidase, leading to increased expression of the phosphaturic hormone FGF23, which in turn prevents activation of the vitamin D pro-hormone.<sup>(3, 4)</sup> The development of rickets in the Hyp mouse model of XLH and in other hypophosphatemic disorders is due to impaired phosphate-mediated hypertrophic chondrocyte apoptosis.<sup>(5, 6)</sup> Of note, however, mice lacking the renal sodium-dependent phosphate transporter IIa (Npt2a) have the same degree of hypophosphatemia as other models, but enhanced 1,25D signaling reverses rickets in these mice despite persistent hypophosphatemia.<sup>(7)</sup> Thus, enhanced 1,25D action can prevent rickets in the setting of hypophosphatemia. In XLH, 1,25D is given along with phosphate supplementation to promote phosphate absorption and prevent hyperparathyroidism due to phosphate monotherapy and hypocalcemia associated with impaired activation of vitamin D.<sup>(1)</sup> This combination therapy improves the growth plate phenotype in mouse models of XLH<sup>(8)</sup> and in affected children.<sup>(2, 9)</sup> While high dose 1,25D and phosphorus can cure osteomalacia,<sup>(10)</sup> this regimen often leads to hypercalcemia, hypercalciuria and nephrocalcinosis,<sup>(11)</sup> and even conventional doses of 1,25D lead to nephrocalcinosis in the setting of phosphate supplementation.<sup>(9)</sup> Thus, there has been significant interest in identifying treatments that reduce the need for oral phosphate by blocking the actions of FGF23, thereby attenuating renal phosphate losses and enhancing 1,25D production.<sup>(12-16)</sup> Investigations in Hyp mice treated for 4 weeks with FGF23 blocking antibodies have demonstrated a 7 fold increase in circulating 1,25D accompanied by improvement in the growth plate and an increase in skeletal ash weight.<sup>(12)</sup> Similarly, interfering with FGF23 signaling by ablating FGFR1,<sup>(17)</sup> FGFR3/4,<sup>(18)</sup> or the FGF23 co-receptor  $\alpha$ -Klotho,<sup>(19)</sup> or treatment with a pan-FGFR inhibitor<sup>(15)</sup> improves the Hyp bone phenotype.

Impairing FGF23 action in XLH leads to increased circulating levels of 1,25D, thus these studies cannot distinguish to what extent the improved phenotype reflects enhanced 1,25D action *versus* decreased renal phosphate losses. Therefore, studies were undertaken to

address the hypothesis that 1,25D attenuates FGF23-independent effects of the PHEX mutation, thus will improve the skeletal phenotype of Hyp mice in the absence of phosphate supplementation. Hyp mice were treated with biweekly high dose 1,25D or daily 1,25D from d2 to d75. Their skeletal phenotype was compared to that of Hyp mice treated with an anti-FGF23 antibody (FGF23Ab), which led to circulating phosphate levels indistinguishable from that of Hyp mice receiving 1,25D alone.

## Materials and Methods

### Animal Studies

Animal studies were approved by the institutional animal care committee. All mice were on a C57BL/6J background, maintained in a virus and parasite free barrier facility and exposed to a 12 hour light/dark cycle. Mice were weaned day 18 onto acidified water and house chow (1% calcium, 0.6% phosphate) and housed in up to 5 mice per cage. Male Hyp mice were subcutaneously injected daily with 1,25D (175 pg/g/day d2-65; 90 pg/g/day d66-75 to maintain normocalcemia, Akorn, Inc.), 3 times per week with an FGF23 blocking antibody (35 mcg/g, Amgen), or biweekly with 1,25D (1.5 ng/g 2x/week) starting on day 2. Wild type and Hyp control male littermates received vehicle or isotype matched antibody (35 mcg/g). Each control or treatment group had at least 5 mice. Primary outcomes were growth and changes in skeletal phenotype; secondary outcomes were alterations in serum mineral ions and hormones. Body weight was monitored on each treatment day. Calcein (30 mg/kg) was injected 2 and 9 days prior to sacrifice day 75. Serum and urine were collected 24 hours after the last treatment. The vertebral column and tail were subjected to x-ray analyses (HP Faxitron #43855A). The length of the lumbar (lumbar levels 1 to 6) and tail (caudal levels 4 to 8) vertebrae was assessed using a standard present on each film.

### Serum and urine parameters

Serum calcium, phosphate, and BUN were measured using a HESKA DRI CHEM 7000 veterinary analyzer. Serum PTH and FGF23 were analyzed using the Mouse Intact PTH 1-84 Kit (Immutopics) and the Mouse C-Terminal FGF23 Kit (Immutopics), respectively. The Phosphorus-Liqui-UV and Creatinine Liquicolor (Endpoint) kits (Stanbio) were used for urine chemistries. Serum 1,25D was measured by competitive ELISA (IdT).

### Histology

Tissues were fixed and processed for paraffin sectioning. Phospho-ERK1/2 (pERK1/2) immunohistochemistry was performed as previously described.<sup>(5, 20)</sup> Sections were blocked with goat anti-mouse Fab fragments (Jackson ImmunoResearch Labs) prior to incubation with anti-SLC34A1 (1:50, Novus Biologicals NBP2-13328). Detection was performed with sodium tyramide amplification (Perkin-Elmer). Sections were blocked with 10% heat inactivated FBS following antigen retrieval and incubated with rabbit anti-Klotho (5 mcg/mL, Abcam ab154163). Signal was detected using goat anti-rabbit HRP (Santa Cruz). *In situ* hybridization was performed as previously reported.<sup>(20)</sup>

### TUNEL assay

The TUNEL assay was performed using an *in situ* cell death detection kit (Roche Diagnostics).<sup>(6)</sup>

### Evaluation of Chondrocyte proliferation

Three hours prior to sacrifice, d35 mice were injected with 250 mcg/g of 5-bromo-2'-deoxyuridine (BrdU) and 30 mcg/g fluorodeoxyuridine (FdU). BrdU was detected using the BrdU detection kit (Invitrogen).

### Cell Culture

Primary chondrocytes were isolated and cultured as previously described.<sup>(6)</sup> Chondrocytes were serum restricted (0.5% FBS) and treated with  $10^{-8}$  M 1,25D 18h prior to exposure to sodium sulfate or sodium phosphate.

### Western Analysis and Subcellular Fractionation

Subcellular fractionation of primary hypertrophic chondrocytes and evaluation of pERK1/2 phosphorylation was performed as previously described.<sup>(20)</sup>

### Real Time PCR

Humeri were dissected free of muscle and connective tissue and following removal of both growth plates, marrow was flushed with phosphate-buffered saline to permit isolation of cortical bone, which was then homogenized in Trizol (Thermo Fisher Scientific). Total RNA was precipitated using 100% ethanol and purified using the RNeasy mini kit (Qiagen). To evaluate PTHrP mRNA expression the head of the humerus was embedded vertically in OCT. Sequential cryosections were stained for 30 seconds in Safranin-O to allow isolation of the peri-articular chondrocytes. Chondrocyte RNA was isolated from the first 50 microns using the RNeasy mini kit (Qiagen). In initial studies, humeri were then reembedded horizontally and cryosectioned to confirm that only sections with periarticular chondrocytes had been included in the RNA isolation. RNA was reverse transcribed with SuperScript™ II (Roche). Quantitative real time-PCR was performed using the QuantiTect SYBR Green RT-PCR kit (Qiagen) on an Opticon DNA engine (MJ Research). Gene expression was normalized to that of a control gene for each sample, using the methods of Livak and Schmittgen.<sup>(5)</sup>

### Micro-computed tomography ( $\mu$ CT)

$\mu$ CT imaging was performed on the mid-diaphysis and distal end of the femur using a high-resolution desktop imaging system ( $\mu$ CT40, Scanco Medical AG, Brüttisellen, Switzerland) as previously described.<sup>(21)</sup> The length of the regions of interest (ROI) was adjusted based on the average femur length for each of the groups. The bone volume fraction of the entire distal femur was also analyzed on contours that were drawn around the outer cortex starting at the top of the trabecular ROI and extending distally to the end of the femur. Thresholds of 316 and 733 mg HA/cm<sup>3</sup> were used for the evaluations of trabecular and cortical bone, respectively, based on adaptive-iterative thresholding (AIT) that was performed on the wild-type group.

## Mechanical testing

Torsion testing was performed rather than 3 point bending due to the short length of the femora of Hyp mice, which did not allow for span lengths long enough to meet the criteria for beam bending. The distal and proximal end of each femur was potted in Polymethyl methacrylate (PMMA). A fixed gage length of 5 mm was maintained between the pots for all specimens. Torsional testing was performed on an electromagnetic mechanical testing machine (ElectroForce 3200, Eden Prairie, MN) with a 0.2 N-m torque sensor. The proximal end of the specimen was held fixed while the distal end was rotated at 1°/sec and rotation and torque data were recorded at 50 Hz. Rotation and torque data were used to calculate maximum torque (N-m), rotational stiffness (N-m/rad), and work to maximum torque (mJ).

## Histomorphometry

Histomorphometry analyses were performed according to the criteria established by the American Society of Bone and Mineral Research.<sup>(22)</sup> Trabecular static, structural and dynamic parameters were measured in the distal femoral metaphysis, 0.2mm below the epiphyseal growth plate, using an Osteomeasure image analyzer (Osteometrics, Atlanta, GA, USA). For cortical bone ten unbroken fields were sequentially selected for cortical osteoid evaluation (magnification 100X). All analyses were performed in a blinded fashion.

## Statistical Analysis

All data shown are reported as mean  $\pm$  standard deviation (SD). One-way ANOVA followed by Fisher's least significant difference (LSD) test was used to analyze significance between all control and treatment groups. Significance was defined as a  $P < 0.05$ .

## Results

### Treatment with 1,25D or FGF23Ab improves serum ions and hormones in Hyp mice

Hyp mice were treated from d2 to d75 with daily 1,25D, FGF23Ab (3x/week), or biweekly high dose 1,25D. All mice had normal serum calcium levels and preserved renal function (Table 1). Nephrocalcinosis was not observed in any of the control or treated mice, nor was a significant increase in BUN (data not shown). Although daily 1,25D treatment of Hyp mice increased calcium levels compared to Hyp control mice, levels were not significantly different from those of WT mice. The treatment groups had similar improvement in serum phosphate levels (Table 1). Both daily 1,25 D and FGF23Ab therapies led to a significant decrease in urinary phosphate excretion, while biweekly 1,25 D treatment did not alter this parameter. All treatments normalized serum PTH levels. Untreated Hyp mice exhibited a significant elevation of serum FGF23 that was further increased by daily and biweekly 1,25D treatment.

Since treatment with the FGF23Ab precludes accurate measurement of serum FGF23 levels, FGF23 mRNA was assessed in the humeral diaphysis of treated mice. While all treatments increased FGF23 mRNA expression, levels in mice treated with daily 1,25 D were significantly higher than those in the other two treatment groups (Fig. 1A). Because of the dramatic increase in FGF23 mRNA expression in the setting of improved renal phosphate reabsorption in mice treated with daily 1,25D and FGF23Ab, immunohistochemistry for

markers of FGF23 signaling was performed on kidneys. Relative to WT kidneys, Hyp control kidneys exhibited decreased immunoreactivity for Npt2a,  $\alpha$ -Klotho, and pERK1/2. Despite increased FGF23 expression, all three treatments restored renal Npt2a immunoreactivity, as well as that of  $\alpha$ -Klotho and pERK1/2 (Fig. 1B). RT-qPCR was performed to determine whether the expression of genes whose ablation increases (DMP1, ENPP1, FAM20c) or decreases (GALNT3, FGFR1c) circulating FGF23 levels was altered<sup>(17, 23–27)</sup> in the bones of treated mice. FGF23Ab treatment normalized DMP1 and FAM20c mRNA levels, while DMP1 and FAM20C were increased in both 1,25D treatment groups. The expression of ENPP1 was increased by all three treatments, whereas that of FGFR1c was normalized (Supplemental Fig. 1). The increase in FAM20C, ENPP1 and DMP1 expression with treatment suggests that enhanced FGF23 signaling may exert a negative feedback loop, inducing the expression of genes that inhibit its expression.

### 1,25D improves growth plate maturation in Hyp mice in the absence of phosphate supplementation

Extracellular phosphate is critical for hypertrophic chondrocyte apoptosis and growth plate maturation.<sup>(5)</sup> However, enhanced 1,25D signaling in Npt2a knockout mice results in normal growth plates in the presence of hypophosphatemia,<sup>(7)</sup> thus we addressed whether 1,25D therapy could exert similar effects in Hyp mice. Growth plate analyses by H&E staining demonstrated that Hyp control mice have dramatically altered morphology compared to WT mice, characterized by a wide, disorganized growth plate accompanied by abnormal morphology of the primary spongiosa (Fig. 2A). All treatments dramatically improved growth plate morphology, restoring the columnar organization of growth plate chondrocytes and improving metaphyseal organization. *In situ* hybridization for collagen type X (ColX), a specific marker for hypertrophic chondrocytes, confirmed that all treatments improved the hypertrophic chondrocyte abnormalities in Hyp mice. In contrast to FGF23Ab and biweekly 1,25 therapies, daily 1,25D resulted in further improvement of growth plate and metaphyseal organization, closely approximating normal morphology (Fig. 2A).

Previous studies have demonstrated that extracellular phosphate induces mitochondrial ERK1/2 phosphorylation,<sup>(20)</sup> leading to hypertrophic chondrocyte apoptosis.<sup>(5, 6)</sup> Hyp control mice exhibited a dramatic decrease in pERK1/2 immunoreactivity, leading to expansion of the hypertrophic chondrocyte layer where pERK1/2 is localized. All treatments increased pERK1/2 immunoreactivity (Fig. 2A) and hypertrophic chondrocyte apoptosis assessed by TUNEL (Fig. 2A and B). Since blocking FGF23 signaling increases 1,25D, we undertook studies to examine whether phosphate-independent 1,25D effects on ERK1/2 phosphorylation could be implicated in these effects. Subcellular fractionation was performed on primary hypertrophic chondrocyte cultures exposed to  $10^{-8}$ M 1,25D for 18 hours prior to 60 minutes treatment with phosphate or sulfate. While 1,25D modestly enhanced cytosolic ERK1/2 phosphorylation in the absence of phosphate, it increased both total and mitochondrial pERK1/2 in the presence and absence of phosphate (Fig. 2C).

To evaluate whether attenuation of rickets translates into an improvement in growth, weights and vertebral and long bone growth were analyzed day 75 (Fig. 2D). Compared to WT mice, Hyp control mice have a significant reduction in body weight, lumbar vertebral height, tail

length, and femur length. Daily 1,25D normalized body weight and lumbar vertebral height, whereas FGF23Ab and biweekly 1,25D increased, but did not normalize lumbar vertebral height and had no effect on body weight (Figure 2D). All treatments increased tail and femur length; however, 1,25D was more effective than FGF23Ab at improving these parameters (Fig. 2D and E).

To determine whether the more beneficial effects of 1,25D treatment on growth were due to altered chondrocyte proliferation, d35 mice were injected with BrdU to evaluate the percentage of proliferating chondrocytes (Supplemental Fig. 2). Unlike biweekly 1,25D, Daily 1,25D and FGF23Ab normalized the impaired chondrocyte proliferation observed in Hyp mice and decreased height of the proliferative chondrocyte zone. Since PTHrP suppresses chondrocyte hypertrophy, expanding the proliferative chondrocyte layer,<sup>(28)</sup> expression of PTHrP mRNA in the peri-articular cartilage of the humeral head was evaluated. Consistent with the effect of these treatments on the height of the proliferative chondrocyte layer, both daily 1,25D and FGF23Ab significantly suppressed peri-articular PTHrP expression, while biweekly 1,25D did not (Supplemental Fig. 2).

### **1,25D and FGF23Ab treatment of Hyp mice improve microarchitecture and biomechanics**

MicroCT and biomechanical analyses were performed to compare the effect of these treatments on bone microarchitecture and strength. Hyp control mice have significantly decreased cortical thickness (Ct.Th) and cortical area fraction (Ct.Ar/Tt.Ar) accompanied by increased cortical porosity, relative to WT mice (Fig. 3A, Supplemental Table 1). While both daily 1,25D and FGF23Ab therapy significantly improved these cortical parameters, biweekly 1,25D treatment improved Ct.Ar/Tt.Ar, but not Ct.Th or cortical porosity. None of the treatments altered trabecular BV/TV. However, images of the distal femurs demonstrate a dramatic increase in mineralization in the daily 1,25D treated mice (Fig. 2D and 3B). Therefore, analysis of total BV/TV (cortical and trabecular) of the femur including the metaphysis, growth plate, and secondary ossification center was performed. While all treatments improved the reduction in total BV/TV observed in the untreated Hyp mice, daily 1,25D had a greater effect than FGF23Ab, which in turn was superior to biweekly 1,25D therapy (Fig. 3A).

Micro-CT evaluation of inferred biomechanical parameters demonstrated a significant reduction in polar moments of inertia (pMOI),  $I_{\min}$  and  $I_{\max}$  in the Hyp mice (Fig. 4A). Daily 1,25D improved the geometry of the femoral diaphysis to the extent that all these parameters were normalized. FGF23Ab treatment significantly improved but did not normalize pMOI and  $I_{\min}$  whereas biweekly 1,25D had no effect on  $I_{\max}$ . To formally characterize biomechanical properties, femurs of d75 control and treated mice were subjected to torsion testing analyses. Relative to WT mice, Hyp control mice have decreased whole-bone strength (Max Torque), stiffness, and toughness (work to Max Torque). All treatments increase strength (Fig. 4B), with daily 1,25D treatment trending towards a more significant increase relative to other treatments (Max Torque  $p=0.06$  vs FGF23Ab;  $p=0.06$  vs biweekly 1,25D) (Fig. 4C). Although both daily 1,25D and FGF23Ab led to a significant improvement in torsional stiffness, only daily and biweekly 1,25D improved toughness (work to Max Torque) (Fig. 4C).

## Effect of 1,25D and FGF23Ab treatment of Hyp mice on histomorphometric parameters

The lack of improvement in trabecular parameters observed in the  $\mu$ CT of treated Hyp mice could represent impaired bone mineralization, little to no improvement in bone formation or a combination thereof. To further evaluate this, histomorphometric analyses were performed (Fig. 5, Supplemental Table 2). A decrease in bone volume/tissue volume (BV/TV) and trabecular number (Tb.N) was observed in the Hyp control mice, accompanied by an increase in trabecular separation (Tb.SP) and osteoid volume (OV/BV). Daily and biweekly 1,25D treatments significantly improved BV/TV and trabecular parameters, while FGF23Ab did not alter this parameter. Daily 1,25D normalized the increased Ct.Th observed in Hyp mice, while neither FGF23Ab nor biweekly 1,25D altered this parameter. Daily 1,25D and FGF23Ab treatment normalized, while biweekly 1,25D significantly decreased OV/BV. The impaired mineral apposition rate (MAR) observed in Hyp mice was not normalized by any treatment. However, unlike Hyp control mice, where no dual calcein labels were observed, MAR was quantifiable in femurs from each of the treated groups, and MS was significantly increased in daily 1,25D treated mice (Supplemental Table 2). To determine if improved mineralization reflects enhanced expression of genes involved in mineralization, RNA was isolated from the humeral diaphysis of treated and control mice d75. The expression of PHOSPHO1,<sup>(29)</sup> ANK,<sup>(30, 31)</sup> and matrix gla protein (MGP)<sup>(32)</sup> was decreased in Hyp control humeri (Supplemental Fig. 3). Both daily and biweekly 1,25D increased the expression of ANK, PHOSPHO1 and MGP, whereas FGF23Ab therapy increased only ANK expression. Expression of sclerostin (SOST), an inhibitor of bone formation that impairs the differentiation and mineralization of cultured osteoblasts, is known to be increased by 1,25D.<sup>(33, 34)</sup> FGF23Ab and biweekly 1,25D normalized the low sclerostin expression observed in untreated Hyp mice, whereas daily 1,25D induced SOST expression to 3 fold above that of WT mice (Supplemental Fig. 3).

## FGF23Ab transiently increases serum 1,25D in Hyp mice

Because daily 1,25D treatment was more effective than FGF23Ab at improving growth plate morphology, growth, skeletal mineralization, and bone volume, serum 1,25D levels were analyzed in Hyp mice treated with the FGF23Ab (Table 2). Day 35 Hyp control mice had lower serum 1,25D levels than WT mice. FGF23Ab treatment resulted in serum 1,25D levels significantly higher than both WT and Hyp control mice day 35 but not day 75.

## All treatments decrease osteocyte apoptosis in Hyp mice

The beneficial effects of 1,25D on the cortical phenotype of the Hyp mice, in the setting of a dramatic increase in FGF23 suggest that the actions of 1,25D may be phosphate- and FGF23- independent. Analyses of cortical bone demonstrated a 30% decrease in osteocyte number in Hyp mice compared to WT mice (Fig. 6A), associated with an increase in osteocyte apoptosis. All treatments normalized osteocyte apoptosis (Fig. 6B).

## Discussion

Current treatment for XLH includes both phosphate supplementation and 1,25D, the latter of which is traditionally used for preventing secondary hyperparathyroidism and promoting intestinal absorption of phosphate.<sup>(11, 35)</sup> Treatment of Hyp mice with phosphate alone has



been shown to improve growth plate thickness,<sup>(36)</sup> but does not normalize the Hyp bone phenotype and does not necessarily increase serum phosphate levels. In contrast, Alzet minipump infusion of 1,25D into Hyp mice for 4 weeks after weaning, along with a diet rich in phosphate, normalizes the growth plate and dramatically improves osteoid thickness,<sup>(10)</sup> suggesting that 1,25D has phosphate-independent or phosphate additive effects on Hyp bone. Because oral phosphate is rapidly cleared and suppresses endogenous 1,25D,<sup>(37)</sup> and because treatment with high dose 1,25D with phosphate leads to hypercalcemia and nephrocalcinosis, we addressed the hypothesis that 1,25D without phosphate supplementation will improve the Hyp skeletal phenotype. Based on the ability of FGF23 blocking antibodies to decrease renal phosphate excretion and increase endogenous 1,25D in Hyp mice, FGF23Ab treated mice were used as controls. FGF23Ab treatment, in contrast to phosphate and 1,25D therapy, offers the distinct advantage of also blocking phosphate-independent actions of FGF23. However, a limitation of the current study is the absence of control groups of hyp mice treated with phosphate alone or phosphate with 1,25D.

Unlike our observations, the studies examining the effects of 28 days of 1,25D and phosphate therapy initiated post weaning<sup>(10)</sup>, did not normalize vertebral length despite a daily 1,25D dose identical to that used in our studies. The more beneficial effects of 1,25D that we observed in the current study may reflect the critical actions of 1,25D on the period of rapid growth prior to weaning, the lack of suppression of endogenous 1,25D by dietary phosphate,<sup>(37)</sup> or differential effects of daily administration *versus* infusion of 1,25D on PTH, FGF23 expression, or bone. Biweekly high dose 1,25D treatment was used in our studies to address whether pharmacological doses of 1,25D are more effective at suppressing PTH levels and attenuate the increase in circulating FGF23 observed with 1,25D. However, the levels of these hormones were indistinguishable in the two 1,25D treatment groups. Despite a more profound increase in bone FGF23 mRNA in the daily 1,25D treated mice, this treatment regimen was uniformly superior to biweekly high dose 1,25D.

Consistent with the role of FGF23 in renal phosphate wasting, treatment strategies directed at blocking FGF23 signaling improve the growth plate phenotype of Hyp mice<sup>(12, 15, 17–19)</sup> with one exception. Blocking FGF23 signaling using a MEK1/2 inhibitor reduced renal phosphate excretion, improved cortical parameters but did not alter the disorganized Hyp growth plate observed.<sup>(16)</sup> This is consistent with our previous findings that MEK1/2 phosphorylation of ERK1/2 is required for phosphate-induced hypertrophic chondrocyte apoptosis;<sup>(5)</sup> thus in spite of the improvement in phosphate homeostasis, phosphate-induction of hypertrophic chondrocyte apoptosis remains blocked in the MEK1/2 inhibitor treated mice.

The current studies demonstrate a specific role for 1,25D in growth plate maturation, where daily treatment with 1,25D alone improved growth plate and metaphyseal morphology more than the FGF23Ab, despite similar levels of circulating calcium, phosphorus and PTH; however, while serum 1,25D levels were increased by FGF23Ab treatment d35, by d75 they were not different from those of WT or Hyp mice. Based on our *in vitro* studies demonstrating that 1,25D increases basal and phosphate-induced mitochondrial ERK1/2 phosphorylation, which is crucial for hypertrophic chondrocyte apoptosis, it is likely that the inability of the FGF23Ab to sustain elevated circulating 1,25D levels contributes to the less

favorable metaphyseal phenotype observed. It is also likely that this underlies the more beneficial effects of 1,25D on Hyp bone. 1,25D therapy is also likely to provide therapeutic benefit in improving growth plate abnormalities and osteomalacia in hypophosphatemic disorders other than XLH. However, the effect of 1,25D observed on bone and osteocyte apoptosis in our studies may be a direct consequence of attenuating FGF23-independent effects of PHEX mutations, thus may not be generalizable to other hypophosphatemic disorders.

Studies by other investigators employing an alternative FGF23 blocking antibody demonstrated that treatment normalized body weight and significantly improved trabecular bone structure.<sup>(12)</sup> However, Hyp mice in those studies were treated for 28 days and had serum 1,25D levels 7 fold higher than Hyp controls, whereas our investigations were performed for 11 weeks and demonstrated increased 1,25D levels after 35 days, but not 75 days of treatment. The inability of the FGF23Ab to sustain increased levels of 1,25D in our studies correlates with the divergence in the growth curve of the FGF23Ab and daily 1,25D treated Hyp mice. The molecular basis for the waning effect of the FGF23Ab on serum 1,25D levels is not known. Future investigations will be required to determine if antibody therapy leads resistance to the effects of the FGF23Ab on the vitamin D 1 $\alpha$ -hydroxylase or the vitamin D 24-hydroxylase. It is notable, however, that the peak increase in 1,25D observed in XLH patients treated with an FGF23 blocking antibody wanes with prolonged duration of treatment<sup>(14)</sup> as does the effect of an FGFR inhibitor in Hyp mice.<sup>(15)</sup>

In the current studies, daily 1,25D treatment normalized body weight, vertebral height, and trabecular separation as well as improved all biomechanical parameters. Both 1,25D regimens improved femur and tail length more so than FGF23Ab. Consistent with the hypothesis that 1,25D has beneficial effects on Hyp bone that are independent of its actions on phosphate homeostasis, FGF23Ab improved but did not normalize growth or trabecular bone structure. Interestingly, daily 1,25D resulted in a decrease in urine phosphate/creatinine, despite marked increases in FGF23 mRNA and plasma levels, and PTH levels that did not differ significantly from those of WT mice. This suggests that 1,25D may impair the biological activity of FGF23 or lead to FGF23 resistance. Notable in this respect, daily 1,25D treated mice have a significant increase in the expression of FAM20C, which phosphorylates FGF23, enhancing its cleavage by preventing glycosylation.<sup>(38)</sup> Thus, it is possible that 1,25D increases the ratio of C-terminal to intact levels of serum FGF23 due to impaired glycosylation. Accumulation of C-terminal fragments could lead to FGF23 resistance by blocking receptor-ligand interactions.<sup>(39)</sup> Alternatively, 1,25D may directly alter FGF23 receptor expression or downstream signaling events.

Daily 1,25D improved bone volume despite an increase in the expression of SOST, an inhibitor of bone formation. All three treatments improved mineralization, associated with increased ANK expression. Corresponding to increased expression of both ANK and PHOSPHO1, increased mineralization was seen in the distal femur of Hyp mice treated daily with 1,25D.

Both daily 1,25D and FGF23Ab treatments improved cortical microarchitecture and whole-bone biomechanical properties, while daily 1,25D normalized the inferred biomechanical

parameters on micro-CT. Consistent with normalization of the moments of inertia, daily 1,25D treatment, unlike FGF23Ab or biweekly 1,25D, significantly increased total cross sectional area (Supplemental Table 1), indicating an increase in periosteal expansion. The difference in inferred biomechanical and whole-bone biomechanical analyses suggests that significant abnormalities in the material properties of bone persist in the daily 1,25D treated mice. This is consistent with transplantation studies and studies in cultured osteoblasts<sup>(40–42)</sup> that demonstrate an intrinsic osteoblast defect in Hyp mice. Although FGF23 impairs mineralization,<sup>(43)</sup> the dramatic increase in FGF23 mRNA in the bones and serum of daily 1,25D treated mice in the setting of improved mineralization suggests that the abnormalities cannot be solely attributed to local production of FGF23. Whether 1,25D modulates the production of ASARM peptides, which have been implicated in the impaired mineralization of Hyp bone,<sup>(44)</sup> or exerts its effects on other PHEX-dependent pathways remains to be determined. While increased FGF23 results in hypophosphatemia and rickets, it is likely that other significant FGF23-independent consequences of PHEX mutations are responsible for the bone abnormalities in XLH. Our studies demonstrate increased strength and improved histomorphometric parameters in Hyp mice with 1,25D therapy, despite a dramatic increase in FGF23. This suggests that 1,25D attenuates FGF23-independent consequences of PHEX mutations that may be critical determinants of skeletal pathology in XLH. Future investigations in mouse models with PHEX-independent FGF23 overexpression will be required to identify skeletal abnormalities specifically due to PHEX ablation *versus* FGF23 excess.

These investigations demonstrate clear beneficial effects of 1,25D on improving growth in the setting of PHEX mutations, thus have clear implications for the treatment of children with XLH, as well as adults whose growth plates are fused. 1,25D without phosphate supplementation, would be anticipated to decrease the risk of nephrocalcinosis in affected individuals. Furthermore, our studies indicate that close attention should be given to repleting 1,25D levels in FGF23Ab-treated subjects when increased circulating 1,25D is not observed. Although there is no consensus regarding indications for treatment of adults with XLH,<sup>(1)</sup> oral phosphate and 1,25D therapy attenuate symptoms and improve histomorphometric parameters in affected individuals.<sup>(45)</sup> Our investigations demonstrate beneficial effects of 1,25D without phosphate supplementation on the microarchitectural and biomechanical properties of Hyp bones. Thus, treatment of XLH with 1,25D alone is likely to offer significant benefit without the complications observed with combined 1,25D and phosphate therapy.<sup>(9, 11)</sup>

## Supplementary Material

Refer to Web version on PubMed Central for supplementary material.

## Acknowledgments

This work was supported by grants from the National Institutes of Health: P30 AR061313, R01 AR061376 (to MBD), T32 DK007529, F32 AR065386, and K08 AR067854 (to ESL), and a Research Fellowship from the European Society for Paediatric Endocrinology (to AR).

## References

1. Carpenter TO, Imel EA, Holm IA, Jan de Beur SM, Insogna KL. A clinician's guide to X-linked hypophosphatemia. *Journal of bone and mineral research : the official journal of the American Society for Bone and Mineral Research*. 2011; 26(7):1381–8.
2. Friedman NE, Lobaugh B, Drezner MK. Effects of calcitriol and phosphorus therapy on the growth of patients with X-linked hypophosphatemia. *The Journal of clinical endocrinology and metabolism*. 1993; 76(4):839–44. [PubMed: 8473393]
3. Liu S, Zhou J, Tang W, Jiang X, Rowe DW, Quarles LD. Pathogenic role of Fgf23 in Hyp mice. *American journal of physiology Endocrinology and metabolism*. 2006; 291(1):E38–49. [PubMed: 16449303]
4. The HYP Consortium. A gene (PEX) with homologies to endopeptidases is mutated in patients with X-linked hypophosphatemic rickets. *Nature genetics*. 1995; 11(2):130–6. [PubMed: 7550339]
5. Miedlich SU, Zalutskaya A, Zhu ED, Demay MB. Phosphate-induced apoptosis of hypertrophic chondrocytes is associated with a decrease in mitochondrial membrane potential and is dependent upon ERK1/2 phosphorylation. *J Biol Chem*. 2010; 285:18270–5. [PubMed: 20404333]
6. Sabbagh Y, Carpenter TO, Demay M. Hypophosphatemia leads to rickets by impairing caspase-mediated apoptosis of hypertrophic chondrocytes. *Proc Natl Acad Sci*. 2005; 102:9637–42. [PubMed: 15976027]
7. Miedlich SU, Zhu ED, Sabbagh Y, Demay MB. The receptor-dependent actions of 1,25-dihydroxyvitamin D are required for normal growth plate maturation in Npt2a knockout mice. *Endocrinology*. 2010; 151(10):4607–12. [PubMed: 20685875]
8. Marie PJ, Travers R, Glorieux FH. Bone response to phosphate and vitamin D metabolites in the hypophosphatemic male mouse. *Calcified tissue international*. 1982; 34(2):158–64. [PubMed: 6282410]
9. Verge CF, Lam A, Simpson JM, Cowell CT, Howard NJ, Silink M. Effects of therapy in X-linked hypophosphatemic rickets. *The New England journal of medicine*. 1991; 325(26):1843–8. [PubMed: 1660098]
10. Marie PJ, Travers R, Glorieux FH. Healing of bone lesions with 1,25-dihydroxyvitamin D3 in the young X-linked hypophosphatemic male mouse. *Endocrinology*. 1982; 111(3):904–11. [PubMed: 6896684]
11. Harrell RM, Lyles KW, Harrelson JM, Friedman NE, Drezner MK. Healing of bone disease in X-linked hypophosphatemic rickets/osteomalacia. Induction and maintenance with phosphorus and calcitriol. *J Clin Invest*. 1985; 75(6):1858–68. [PubMed: 3839245]
12. Aono Y, Yamazaki Y, Yasutake J, Kawata T, Hasegawa H, Urakawa I, et al. Therapeutic effects of anti-FGF23 antibodies in hypophosphatemic rickets/osteomalacia. *Journal of bone and mineral research : the official journal of the American Society for Bone and Mineral Research*. 2009; 24(11):1879–88.
13. Carpenter TO, Imel EA, Ruppe MD, Weber TJ, Klausner MA, Wooddell MM, et al. Randomized trial of the anti-FGF23 antibody KRN23 in X-linked hypophosphatemia. *J Clin Invest*. 2014; 124(4):1587–97. [PubMed: 24569459]
14. Imel EA, Zhang X, Ruppe MD, Weber TJ, Klausner MA, Ito T, et al. Prolonged Correction of Serum Phosphorus in Adults With X-Linked Hypophosphatemia Using Monthly Doses of KRN23. *The Journal of clinical endocrinology and metabolism*. 2015; 100(7):2565–73. [PubMed: 25919461]
15. Wöhrle S, Henninger C, Bonny O, Thuery A, Beluch N, Hynes NE, et al. Pharmacological inhibition of fibroblast growth factor (FGF) receptor signaling ameliorates FGF23-mediated hypophosphatemic rickets. *Journal of bone and mineral research : the official journal of the American Society for Bone and Mineral Research*. 2013; 28(4):899–911.
16. Zhang MY, Ranch D, Pereira RC, Armbrrecht HJ, Portale AA, Perwad F. Chronic inhibition of ERK1/2 signaling improves disordered bone and mineral metabolism in hypophosphatemic (Hyp) mice. *Endocrinology*. 2012; 153(4):1806–16. [PubMed: 22334725]
17. Xiao Z, Huang J, Cao L, Liang Y, Han X, Quarles LD. Osteocyte-specific deletion of Fgfr1 suppresses FGF23. *PLoS one*. 2014; 9(8):e104154. [PubMed: 25089825]

18. Li H, Martin A, David V, Quarles LD. Compound deletion of Fgfr3 and Fgfr4 partially rescues the Hyp mouse phenotype. *American journal of physiology Endocrinology and metabolism*. 2011; 300(3):E508–17. [PubMed: 21139072]
19. Brownstein CA, Zhang J, Stillman A, Ellis B, Troiano N, Adams DJ, et al. Increased bone volume and correction of HYP mouse hypophosphatemia in the Klotho/HYP mouse. *Endocrinology*. 2010; 151(2):492–501. [PubMed: 19952276]
20. Liu ES, Zalutskaya A, Chae BT, Zhu ED, Gori F, Demay MB. Phosphate interacts with PTHrP to regulate endochondral bone formation. *Endocrinology*. 2014; 155(10):3750–6. [PubMed: 25057796]
21. Zhu ED, Louis L, Brooks DJ, Bouxsein ML, Demay MB. Effect of bisphosphonates on the rapidly growing male murine skeleton. *Endocrinology*. 2014; 155(4):1188–96. [PubMed: 24422540]
22. Dempster DW, Compston JE, Drezner MK, Glorieux FH, Kanis JA, Malluche H, et al. Standardized nomenclature, symbols, and units for bone histomorphometry: a 2012 update of the report of the ASBMR Histomorphometry Nomenclature Committee. *Journal of bone and mineral research : the official journal of the American Society for Bone and Mineral Research*. 2013; 28(1):2–17.
23. Martin A, Liu S, David V, Li H, Karydis A, Feng JQ, et al. Bone proteins PHEX and DMP1 regulate fibroblastic growth factor Fgf23 expression in osteocytes through a common pathway involving FGF receptor (FGFR) signaling. *FASEB journal : official publication of the Federation of American Societies for Experimental Biology*. 2011; 25(8):2551–62. [PubMed: 21507898]
24. Wang X, Wang S, Li C, Gao T, Liu Y, Rangiani A, et al. Inactivation of a novel FGF23 regulator, FAM20C, leads to hypophosphatemic rickets in mice. *PLoS genetics*. 2012; 8(5):e1002708. [PubMed: 22615579]
25. Feng JQ, Ward LM, Liu S, Lu Y, Xie Y, Yuan B, et al. Loss of DMP1 causes rickets and osteomalacia and identifies a role for osteocytes in mineral metabolism. *Nature genetics*. 2006; 38(11):1310–5. [PubMed: 17033621]
26. Lorenz-Depiereux B, Schnabel D, Tiosano D, Hausler G, Strom TM. Loss-of-function ENPP1 mutations cause both generalized arterial calcification of infancy and autosomal-recessive hypophosphatemic rickets. *American journal of human genetics*. 2010; 86(2):267–72. [PubMed: 20137773]
27. Ichikawa S, Sorenson AH, Austin AM, Mackenzie DS, Fritz TA, Moh A, et al. Ablation of the Galnt3 gene leads to low-circulating intact fibroblast growth factor 23 (Fgf23) concentrations and hyperphosphatemia despite increased Fgf23 expression. *Endocrinology*. 2009; 150(6):2543–50. [PubMed: 19213845]
28. Lee K, Lanske B, Karaplis AC, Deeds JD, Kohno H, Nissenson RA, et al. Parathyroid hormone-related peptide delays terminal differentiation of chondrocytes during endochondral bone development. *Endocrinology*. 1996; 137(11):5109–18. [PubMed: 8895385]
29. Roberts S, Narisawa S, Harmey D, Millan JL, Farquharson C. Functional involvement of PHOSPHO1 in matrix vesicle-mediated skeletal mineralization. *Journal of bone and mineral research : the official journal of the American Society for Bone and Mineral Research*. 2007; 22(4):617–27.
30. Wang W, Xu J, Du B, Kirsch T. Role of the progressive ankylosis gene (ank) in cartilage mineralization. *Molecular and cellular biology*. 2005; 25(1):312–23. [PubMed: 15601852]
31. Wennberg C, Hessle L, Lundberg P, Mauro S, Narisawa S, Lerner UH, et al. Functional characterization of osteoblasts and osteoclasts from alkaline phosphatase knockout mice. *Journal of bone and mineral research : the official journal of the American Society for Bone and Mineral Research*. 2000; 15(10):1879–88.
32. Murshed M, Schinke T, McKee MD, Karsenty G. Extracellular matrix mineralization is regulated locally; different roles of two gla-containing proteins. *The Journal of cell biology*. 2004; 165(5): 625–30. [PubMed: 15184399]
33. Kogawa M, Wijenayaka AR, Ormsby RT, Thomas GP, Anderson PH, Bonewald LF, et al. Sclerostin regulates release of bone mineral by osteocytes by induction of carbonic anhydrase 2. *Journal of bone and mineral research : the official journal of the American Society for Bone and Mineral Research*. 2013; 28(12):2436–48.

34. Wijenayaka AR, Yang D, Prideaux M, Ito N, Kogawa M, Anderson PH, et al. 1alpha,25-dihydroxyvitamin D3 stimulates human SOST gene expression and sclerostin secretion. *Molecular and cellular endocrinology*. 2015; 413:157–67. [PubMed: 26112182]
35. Glorieux FH, Marie PJ, Pettifor JM, Delvin EE. Bone response to phosphate salts, ergocalciferol, and calcitriol in hypophosphatemic vitamin D-resistant rickets. *The New England journal of medicine*. 1980; 303(18):1023–31. [PubMed: 6252463]
36. Marie PJ, Travers R, Glorieux FH. Healing of rickets with phosphate supplementation in the hypophosphatemic male mouse. *J Clin Invest*. 1981; 67(3):911–4. [PubMed: 6259210]
37. Meyer RA Jr, Meyer MH, Morgan PL. Effects of altered diet on serum levels of 1,25-dihydroxyvitamin D and parathyroid hormone in X-linked hypophosphatemic (Hyp and Gy) mice. *Bone*. 1996; 18(1):23–8. [PubMed: 8717533]
38. Tagliabracci VS, Engel JL, Wiley SE, Xiao J, Gonzalez DJ, Nidumanda Appaiah H, et al. Dynamic regulation of FGF23 by Fam20C phosphorylation, GalNAc-T3 glycosylation, and furin proteolysis. *Proc Natl Acad Sci U S A*. 2014; 111(15):5520–5. [PubMed: 24706917]
39. Goetz R, Nakada Y, Hu MC, Kurosu H, Wang L, Nakatani T, et al. Isolated C-terminal tail of FGF23 alleviates hypophosphatemia by inhibiting FGF23-FGFR-Klotho complex formation. *Proc Natl Acad Sci U S A*. 2010; 107(1):407–12. [PubMed: 19966287]
40. Ecarot B, Glorieux F, Desbarats M, Travers R, Labelle L. Defective bone formation by Hyp mouse bone cells transplanted into normal mice: evidence in favor of an intrinsic osteoblast defect. *Journal of bone and mineral research : the official journal of the American Society for Bone and Mineral Research*. 1992; 7:215–20.
41. Miao D, Bai X, Panda D, McKee M, Karaplis A, Goltzman D. Osteomalacia in Hyp mice is associated with abnormal Phex expression and with altered bone matrix protein expression and deposition. *Endocrinology*. 2001; 142:926–39. [PubMed: 11159866]
42. Liu S, Tang W, Zhou J, Vierthaler L, Quarles LD. Distinct roles for intrinsic osteocyte abnormalities and systemic factors in regulation of FGF23 and bone mineralization in Hyp mice. *American journal of physiology Endocrinology and metabolism*. 2007; 293(6):E1636–44. [PubMed: 17848631]
43. Sitara D, Kim S, Razzaque MS, Bergwitz C, Taguchi T, Schuler C, et al. Genetic evidence of serum phosphate-independent functions of FGF-23 on bone. *PLoS genetics*. 2008; 4(8):e1000154. [PubMed: 18688277]
44. Bresler D, Bruder J, Mohnike K, Fraser WD, Rowe PS. Serum MEPE-ASARM-peptides are elevated in X-linked rickets (HYP): implications for phosphaturia and rickets. *The Journal of endocrinology*. 2004; 183(3):R1–9. [PubMed: 15590969]
45. Sullivan W, Carpenter T, Glorieux F, Travers R, Insogna K. A prospective trial of phosphate and 1,25-dihydroxyvitamin D3 therapy in symptomatic adults with X-linked hypophosphatemic rickets. *The Journal of clinical endocrinology and metabolism*. 1992; 75(3):879–85. [PubMed: 1517380]

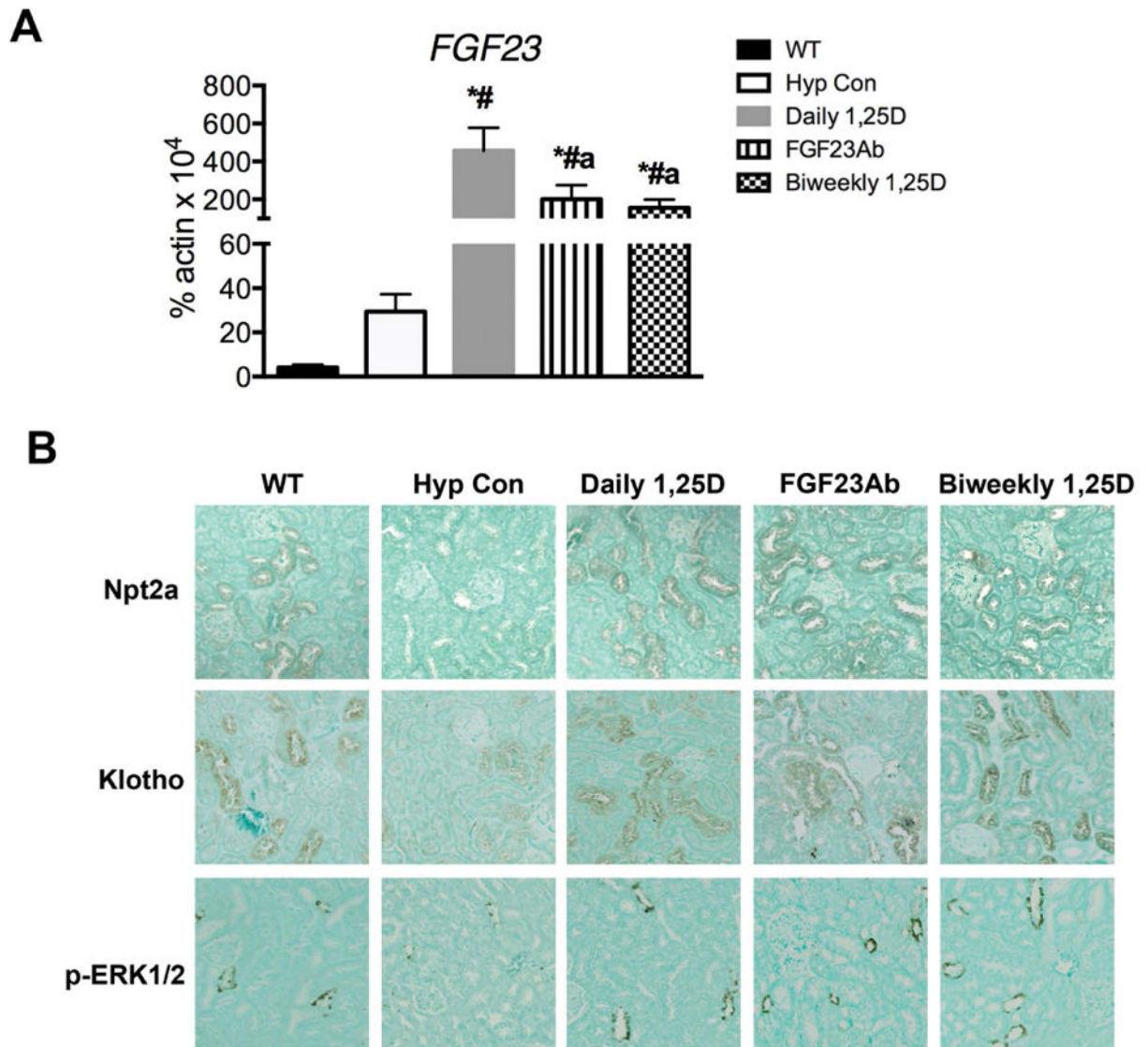


**Fig 1.** 1,25D and FGF23Ab treatment increase FGF23 mRNA levels and restore renal Npt2a,  $\alpha$ -Klotho and pERK1/2 immunoreactivity in Hyp mice. A. RNA isolated from the humeral diaphysis of d75 mice was subjected to RT-qPCR for evaluation of FGF23 mRNA levels. All treatments dramatically increased long bone FGF23 mRNA expression. Data, normalized for actin in each sample represents RNA isolated from 3 mice per genotype/treatment group. B. Immunohistochemical evaluation of Npt2a,  $\alpha$ -Klotho and pERK1/2 was performed on sections of kidneys obtained d75, 24h after the final treatment. All treatments increased Npt2a,  $\alpha$ -Klotho and pERK1/2 immunoreactivity relative to untreated Hyp control mice. Data are representative of that obtained from 3 mice per genotype/treatment group. \* = p value <0.05 vs WT, # = p value <0.05 vs Hyp Con (Hyp control), a = p value <0.05 vs Daily 1,25D.

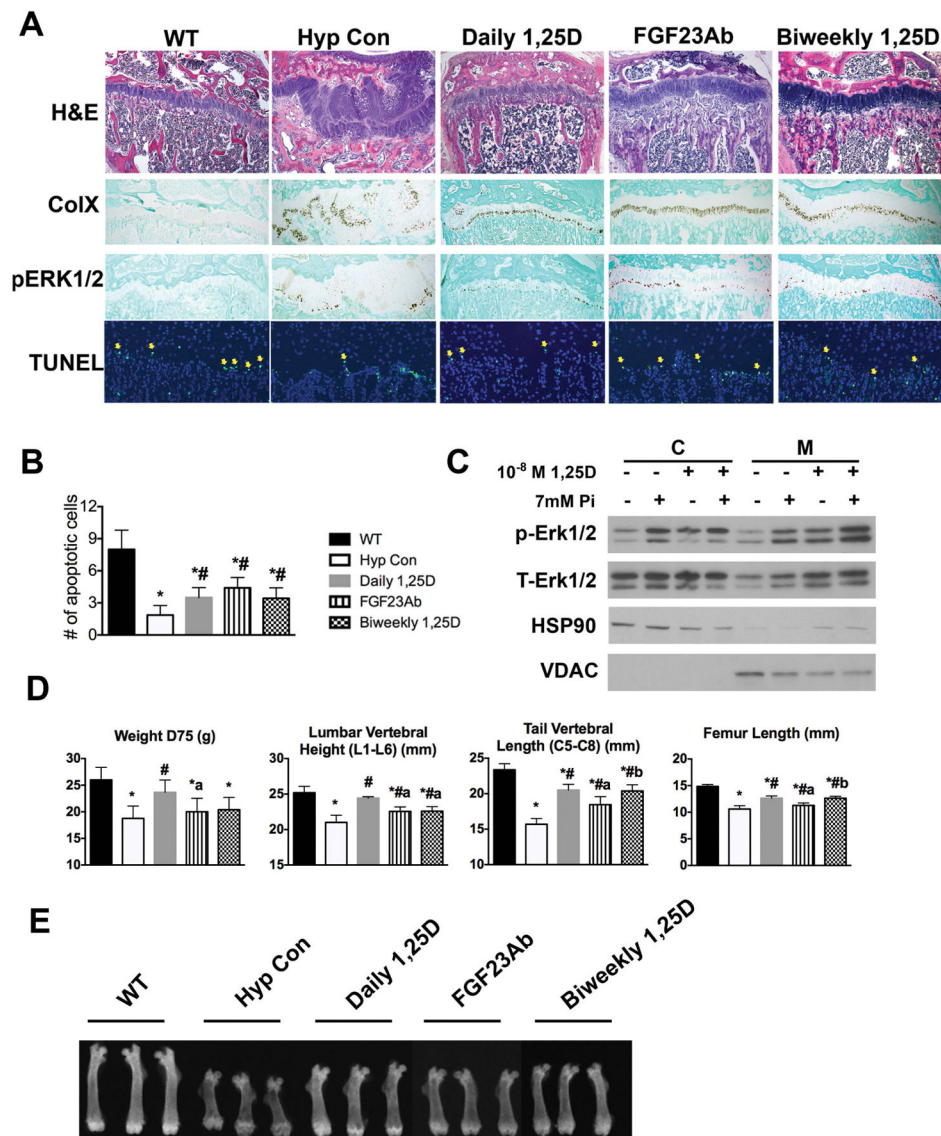


**Fig. 2.** 1,25D and FGF23Ab effects on growth plate and metaphyseal morphology and growth in Hyp mice. **A.** H&E, Col X *in situ* hybridization, pERK1/2 immunoreactivity and TUNEL labeling of the growth plates of d75 mice. Yellow arrows indicate TUNEL labeled hypertrophic chondrocytes. Data are representative of 3 mice per genotype/treatment group. **B.** The number of TUNEL labeled nuclei in the last two rows of the hypertrophic chondrocyte layer was quantitated. Data are representative of 3 mice per genotype/treatment group. **C.** 1,25D increases basal and phosphate-induced mitochondrial pERK1/2. Subcellular fractionation of hypertrophic chondrocytes treated with 10<sup>-8</sup> M 1,25D prior to addition of 7mM sodium sulfate (-) or sodium phosphate (Pi). HSP90 is used as a cytosolic control and VDAC as a mitochondrial control. Data are representative of that obtained from 3 independent chondrocyte preparations. **D.** Weight, lumbar vertebral height, tail length and femur length of d75 mice. Data are representative of that obtained from 3 to 5 mice per



genotype/treatment group. E. Radiographs of representative femurs. \* =p value <0.05 vs WT, # =p value <0 vs Hyp Con, a =p value <0.05 vs Daily 1,25D, b =p value <0.05 vs FGF23Ab.

Author Manuscript

Author Manuscript

Author Manuscript

Author Manuscript

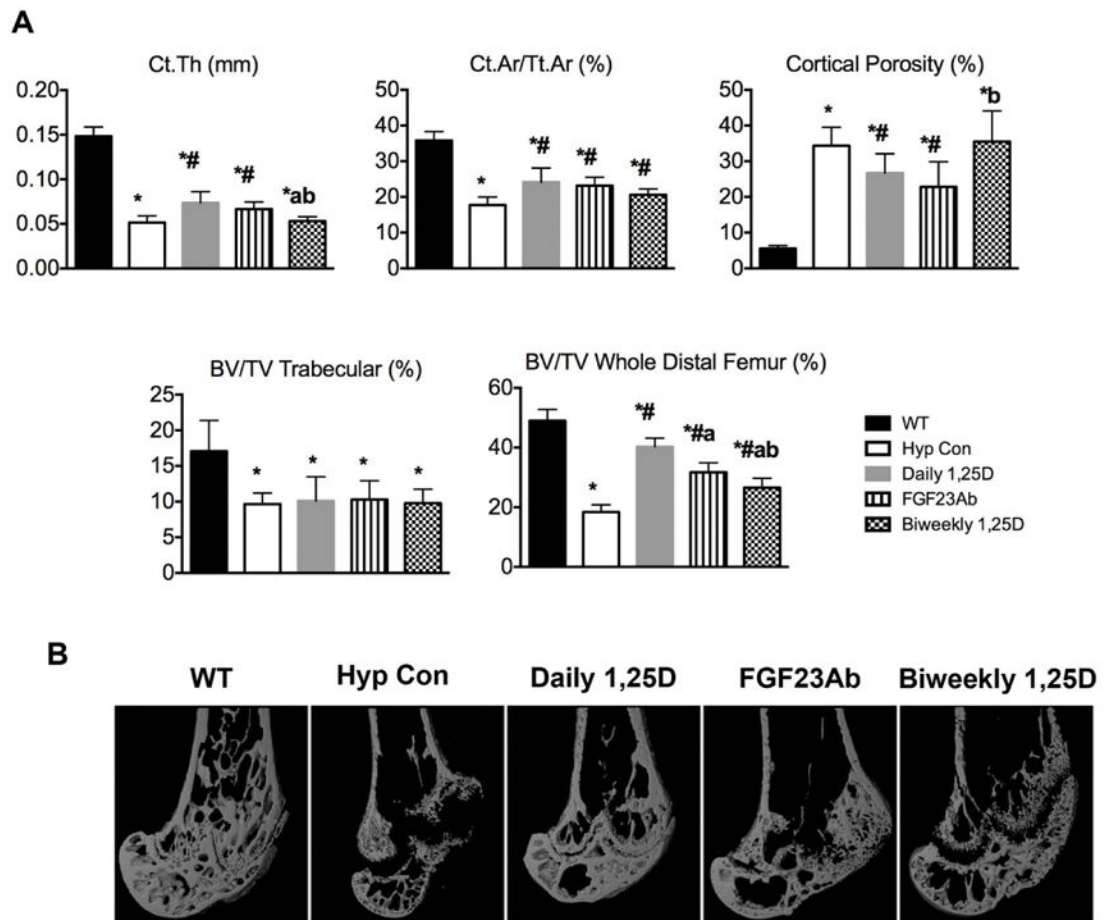


**Fig. 3.** 1,25D and FGF23Ab treatment improve microarchitecture. A. MicroCT scans were performed on femurs isolated from d75 mice. Ct. Th, cortical thickness; Ct.Ar/Tt.Ar, Cortical Area/Total Area; BV/TV, Bone Volume/Tissue Volume. Data represent that obtained from 5 mice per genotype/treatment group. \* =p value <0.05 vs WT, # =p value <0.05 vs Hyp Con, a =p value <0.05 vs Daily 1,25D, b =p value <0.05 vs FGF23Ab. B. Representative images of microCT scans are shown.

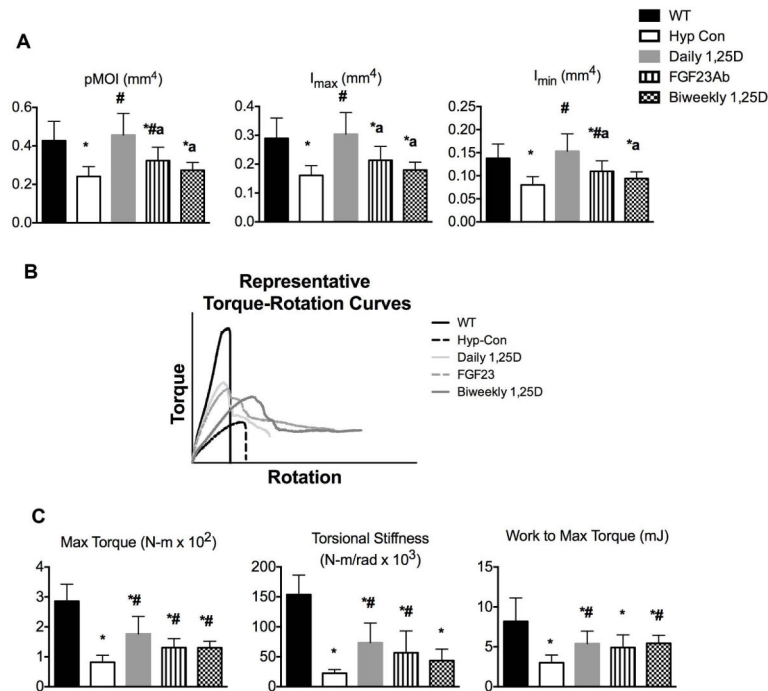


**Fig. 4.** 1,25D and FGF23Ab improve bone strength. A. Inferred biomechanical parameters from microCT analyses. pMOI, polar moment of inertia. B. Torsion testing was performed on d75 femurs. Representative torque rotation curves are shown. C. Torsion testing evaluation of whole-bone strength (Max Torque), stiffness and toughness (work to Max Torque). Data represent that obtained from 5 mice per genotype/treatment group. \* =p value <0.05 vs WT, # =p value <0.05 vs Hyp Con, a =p value <0.05 vs Daily 1,25D.

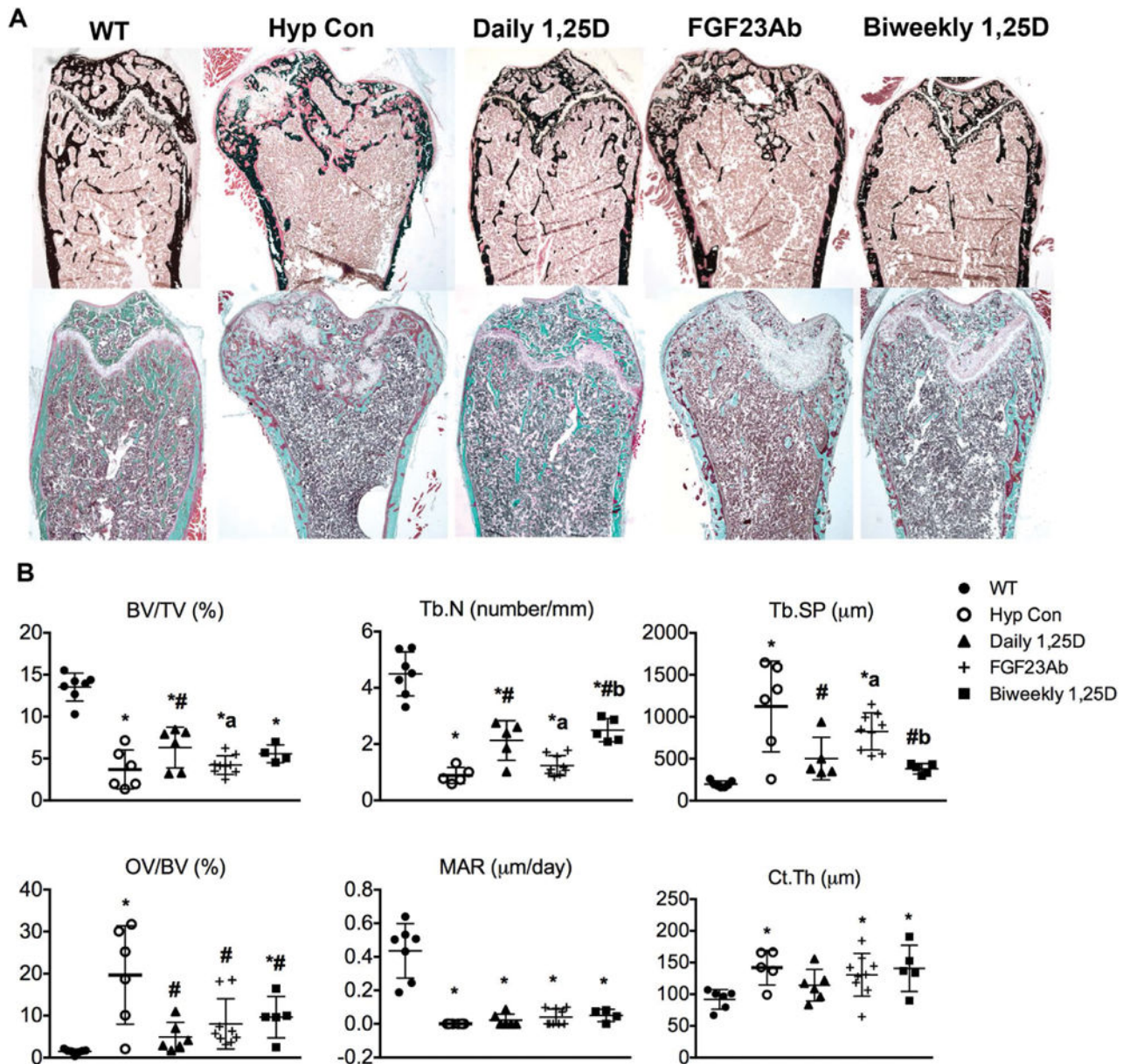


**Fig. 5.** 1,25D and FGF23Ab improve mineralization. A. von Kossa and trichrome staining of the distal femur of d75 mice. B. Histomorphometric parameters. BV/TV, Bone Volume/Tissue Volume; Tb.N, Trabecular Number; Tb.Sp., Trabecular Separation; OV/BV, Osteoid Volume/Tissue Volume; MAR, Mineral Apposition Rate; Ct.Th., Cortical Thickness. Data are representative of that obtained from 5–8 mice per treatment/genotype. \* = p value <0.05 vs WT, # = p value <0.05 vs Hyp Con, a = p value <0.05 vs Daily 1,25D, b = p value <0.05 vs FGF23Ab.

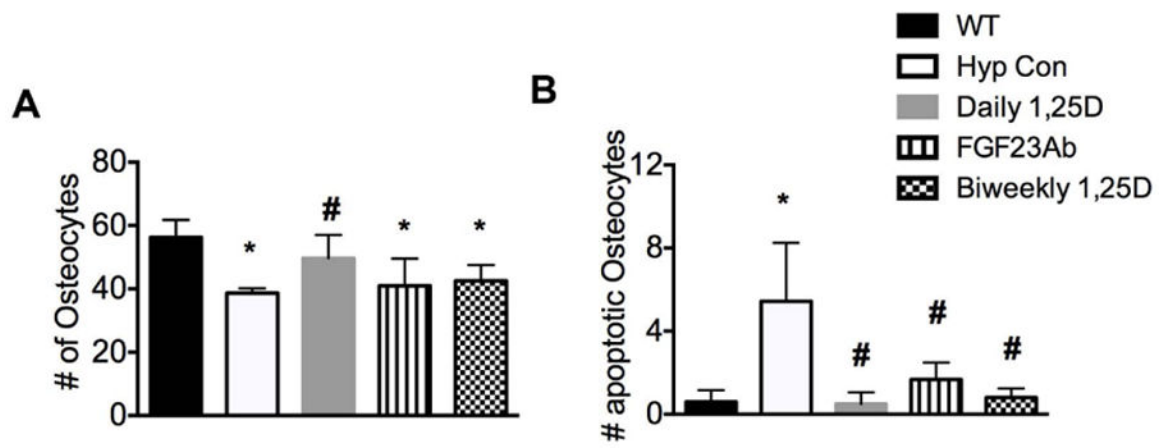


**Fig. 6.**

Osteocyte apoptosis is increased in Hyp cortical bone. A. The number of osteocytes 4 to 5mm proximal and contralateral to the tibiofibular junction in d75 mice was quantitated. Data represent that obtained from three mice per genotype/treatment group. B. Osteocyte apoptosis was quantitated in the tibial cortex of d75 mice. Data represent that obtained from 3 mice per genotype/treatment group. \* =p value <0.05 vs WT, # =p value <0.05 vs Hyp Con

Mineral ion and hormone levels were measured in d35 mice, 24h after the final treatment.

**Table 1**

	WT	Hyp Con	Daily 1,25D	FGF23Ab	Biweekly 1,25D
<b>Ca (mg/dL)</b>	9.6±0.3	9.2±0.4	10.2±0.3 #	9.4±0.3	9.9±0.3
<b>BUN (mg/dL)</b>	28.9±6.9	16.5±4.7 *	35.8±9.0 #	24.5±10.5	15.3±2.0 <sup>a</sup>
<b>Pi (mg/dL)</b>	11.5±0.9	5.1±0.6 *	7.0±0.4 <sup>a</sup> #	6.7±0.2 <sup>a</sup> #	6.7±1.1 <sup>a</sup> #
<b>UrP/UrCr</b>	8.0±2.7	10.4±3.6 *	5.6±0.8 <sup>a</sup> #	4.3±2.0 <sup>a</sup> #	9.5±4.3 <sup>b</sup>
<b>PTH(pg/mL)</b>	149±67	426±145 *	206±82 #	130±55 #	142±70 #
<b>FGF23 (pg/mL)</b>	508 ±231	4250 ± 773	9137±1142 <sup>a</sup> #	N/A	8030±1784 <sup>a</sup> #

Data represent the mean and SD of that obtained from at least 3 mice per genotype/treatment group.

Hyp Con: Hyp control mice, UrP/UrCr: Urine phosphate/Urine creatinine.

\* p value <0.05 vs WT,

# p value <0.05 vs Hyp Con,

<sup>a</sup> p value <0.05 vs Daily 1,25D,

<sup>b</sup> p value <0.05 vs FGF23Ab.

**Table 2**

FGF23Ab transiently increases serum 1,25D. Serum levels of 1,25D were evaluated in d35 and d75 mice in the treatment groups indicated.

	WT	Hyp Con	FGF23Ab
d35	68.3±8.1	43.6±12.2 *	108.6±20.1 *#
d75	35.8±11.8	42.6±11.5	55.2±13.0

Data represent the mean and SD of that obtained from 5 mice per genotype/treatment group.

\* p value <0.05 vs WT,

# p value <0.05 vs Hyp Con.